

## FRACTAL ANALYSIS IN COMPLEX ARTERIAL NETWORK OF PULMONARY X-RAYS IMAGES

Mihai-Virgil NICHITA<sup>1,2</sup>, Viorel-Puiu PAUN<sup>3\*</sup>

*The fractal dimension of a complex arterial network from pulmonary X-rays images has been analyzed. The radiographies was processed in MATLAB R2017a to only highlight the arteries extracted from the context of a complete lung. In addition to this, the comparison between the results obtained in MATLAB environment and Harmonic and Fractal Image Analyzer Demo version 5.5.30 software did not show any significant difference.*

**Keywords:** chaos theory, arterial network, fractal dimension, fractal analysis, respiratory diseases

### 1. Introduction

As time went on, classic geometry seemed to be overcome when details are taken into discussion. Areas of activity such as medicine, chemistry or physics demand high resolution in measurements to provide the most reliable result for an activity—a specialized research, successfully performed in any of the cited domains.

The Chaos theory and fractals analysis makes comprehensible the intricate systems behavior or unpredictable reactions occurrence to scale change and studies extensive and complicated systems, named complex systems.

Based on knowledge from chaos theory according to which a small error introduced in the incipient phase of an analysis can provide totally different conclusions at the end of the process, MATLAB R2017a software was used to reduce the noise that affects the image as much as possible owing to its ability to work with pixel arrays, fact that allows for detailed image analysis and therefore smaller parts of the network can be considered.

In this paper a method of analyzing human X-rays will be presented using a few software algorithms to process the images. Today, helped by X-ray technology, we can study organs due to the differences that occur in the

---

<sup>1</sup> The Special Telecommunications Service, Bucharest, Romania

<sup>2</sup> Student at the Doctoral School of the Applied Sciences Faculty, University POLITEHNICA of Bucharest, Romania

<sup>3</sup> Professor at the Physics Department, Faculty of Applied Sciences, University POLITEHNICA of Bucharest, Romania

\*corresponding author: e-mail: paun@physics.pub.ro

propagation of these rays through various environments that make up the tissue of the human body.

In the first chapter of this work a short introduction in fractal theory will be presented for better understanding on why certain structures of human body can be approached using fractal geometry.

The second chapter will show the actual application of fractal theory and chaos theory in the analysis of various radiographs of human tissues such as the lungs and the vascular system associated.

In fact, fractals can be applied in all chaotic representations, difficult to describe at first glance, but using computer science facilities scientists of our days can achieve impressive conclusions. In the final chapters of the paper some conclusions will be presented to highlight the main results of this paper and propose new research topics based on the work carried out to achieve this goal.

## **2. Fractals and fractal analysis**

The size of an object describes the way it fills the space and by consequence the way it can be measured.

Due to its straight lines and smooth surfaces, Euclidean geometry cannot represent the geometry of complicated forms. For this purpose fractal geometry was defined by Benoit Mandelbrot (1924-2010), the Swedish mathematician of French origins, by publishing the reference work "Fractal Geometry of Nature" in 1977 [1]. Helped by the infinitely detailed coastlines, the fractal geometry can offer new topics to be analyzed by mathematicians and new ways for programmers to develop novel virtual environments similar to reality.

A fractal has the following property: its parts have identical look with the whole, but less after simple changes are applied. Moreover, if the fractal is composed of a certain number of copies, each reduced to a certain scale and possibly slightly modified, it will be called self-similar. The importance of self-similarity property is significant because most of the natural objects are self-similar.

Changes suffered by the whole object to obtain the new form can be described with projective transformations which are defined as combinations of resizing, translations and rotations of space.

Since the fractals were discovered, the characterization of a shape by its topological dimension, expressed by a whole number, has proven to be insufficient. An eloquent example of this is the Koch Curve. It presents a strange phenomenon, as it consists of a multitude of points, of area 0 but of infinite perimeter, and the length increases  $\frac{4}{3}$  times at each iteration. Therefore, using Euclidean geometry, we will not be able to quantify the size of Koch's curve. It is

not appropriate to look at Koch's curve as a Euclidean object of magnitude 1, as it has an infinite perimeter but not a 2-dimensional because its area is 0.

Thus, the notion of fractal dimension will be introduced, this being expressed by a rational number. Besides, the very notion of fractal is closely related to the one of fractal dimension. A fractal is a figure whose fractal dimension is strictly larger than the topological dimension.

The dependence of the scale used makes fractal objects difficult to measure in the context of classical geometry. Their physical properties (length, area, volume) depend on resolution representation.

Around 1914, Hausdorff defines a new concept of topological spaces, suggesting that the fractal dimension is proportional to the minimum number of spheres, of given radius required to cover the measured object.

Nowadays, to make computer processing much easier, cubes or rectangular surfaces are used.

Thus, to cover a curve of length 1,  $N(s) = 1 / s$  cubes of side  $s$  are required. To cover a surface area of 1,  $N(s) = 1 / s^2$  cubes of side  $s$  are required and, finally, to cover a volume cube of 1,  $N(s) = 1 / s^3$  cubes of side  $s$  are required.

So the Hausdorff dimension [2], also known as the Hausdorff-Besicovich size, is defined by the most effective coverage, as follows:

*Considering  $d, s$  from  $R$  and  $N(s)=f(d)*s^d$  a set of functions such that  $N(s)$  is the number of spheres of  $s$  diameter (cubes of  $s$  side) needed to cover the given set  $F$ . Then there is a unique real value  $d=D_H$ , called the Hausdorff dimension of  $F$ , so that:*

$$d > D_H \Rightarrow N(s) \rightarrow 0 \quad (1)$$

The measure that characterizes an object with the Hausdorff dimension is given by the relationship:

$$N(s) * s^{D_H} \quad (2)$$

Initially, Mandelbrot defined the fractals, as they were called (fractus), as those shapes with infinite details at any level. Then he came back on defining the concept of self-similarity, stating that fractals are those forms made up of similar parts, in a certain way, with the whole. Finally he has given a new definition, the only formal form by which the fractals are the shapes whose Hausdorff dimension exceeds strictly the topological dimension:  $D_H > D_T$ .

A fundamental feature of fractals is similarity. Mandelbrot noticed that a coastline, seen from the plane, looks like a straight line, but as it is as we approach it, it becomes increasingly fragmented, more delicate, at any level of detail that resembles the whole. Starting from this observation, Mandelbrot gave a first definition of fractals as those objects made up of their children on another scale.

Types of similarity:

- self-similarity (perfect similarity) - the object is made up of his copies, at different scales of representation. In general, this kind of similarity is encountered at artificial fractals, computer generated and has major advantages in applications such as fractal compression;
- similarity on portions - the object is made up of similar copies. This kind of similarity is encountered both in artificial fractals and in natural fractals. Similarity on portions was observed by Jaquin, who built on it a powerful image compression algorithm based on fractal techniques, whose results were encouraging both for artificial images, as well as for real ones;
- Brownian - the object is fragmented into random parts, showing details at each level. Brownian similarity is encountered in plasma-fractals, used in creation real coastlines or landscapes.

An important category of fractal shapes studied by fractal geometry is represented by artificial fractals (computer generated), (Sierpinski's triangle, Koch coastline, Cantor's dust, Heighway's dragon, and many others). Starting from the idea that the fractal dimension aims at evaluating the degree of fragmentation of an object, for the category of self-assimilated fractal objects there is a simple interpretation of formulas:

$$Df = \frac{\log(\text{Number of self - similar copies})}{\log(\text{contraction factor})} \quad (3)$$

Therefore, the self-dimensional dimension measures the invariance (scale) of the object  $F$  to different operations (resizing, translation, rotation). This calculation method assumes that the object under consideration is self-similar. However, there is a generalization, called self-affinity, which denotes it statistical scale invariance.

The fractal analysis and adjacent calculus programs, specifically associated with point requirements, have been developed for important topics in physics [3, 4], medicine [5, 6] and materials science [7-10], with focus on nanomaterials [11, 12]. Calculating fractal dimension and other intrinsic parameters and concepts in the theory of complexity such as Lyapunov exponents, attractors (strange attractor, the Hénon attractor), attractor reconstruction (phase space) and new predictive models are the subject of well-known articles [13] and books, in the community of specialists. The clinical part and the radiologies evaluated in the article are based on the work of the authors, experts on lung and brain diseases, detection, amelioration and healing [14-16].

### 3. Complex networks analysis in the human body

There are several networks in the human body which, by distributing some commands or substances, help the body to function properly. Among these we can mention: the nervous system, the vascular system, the capillary network of the lungs, etc.

Analysis of such networks is difficult to achieve using classical geometry due to irregular and varied form from individual to individual. Therefore, the application of fractal geometry is recommended when it is desired to find out their shape or size.

Not only networks can be analyzed using fractal geometry. For example, in surgery, the shape or lengths of organs or tumors are valuable pieces of information in the diagnosis and treatment of diseases.

In this paper the vascular network of the lungs will be presented starting from a pulmonary radiograph. In Figure 1, the lung radiograph on which the fractal analysis was made is depicted.

The entire protocol of processing and analyzing the information contained in pulmonary radiograph was performed with MATLAB R2017a and then Harmonic and Fractal Image Analyser Demo version 5.5.30 was used to compare and check the results.

The texture of the lungs is light, porous, and spongy, the lung floats in the water and when handled at the fingers they feel creped, due to the presence of air in the alveoli. It is also very elastic, hence the state of retraction of these organs appears when they are removed from the closed thoracic cavity. Its surface is smooth, glowing in many polyhedral areas, which indicate the lobules of the organ: numerous fine strips cross each of these areas.



Fig. 1. The lung radiograph on which the fractal analysis was made

Firstly, due to the lung texture, which has a luminance close to that of the arteries, it was necessary to remove it from the radiography and keep the arteries to have a more accurate measurement.

Secondly, as a processing step before analysis, it is necessary to make the background uniform and then convert the image into a binary image. To make the background illumination uniform, an approximation of the background as a separate image and then a subtraction of the background as a separate image are needed [17].

To create a background approximation image, all the pixels which represent the lungs must be removed from the picture using morphological opening. This kind of operation has the effect of removing objects that cannot completely contain the structuring element.

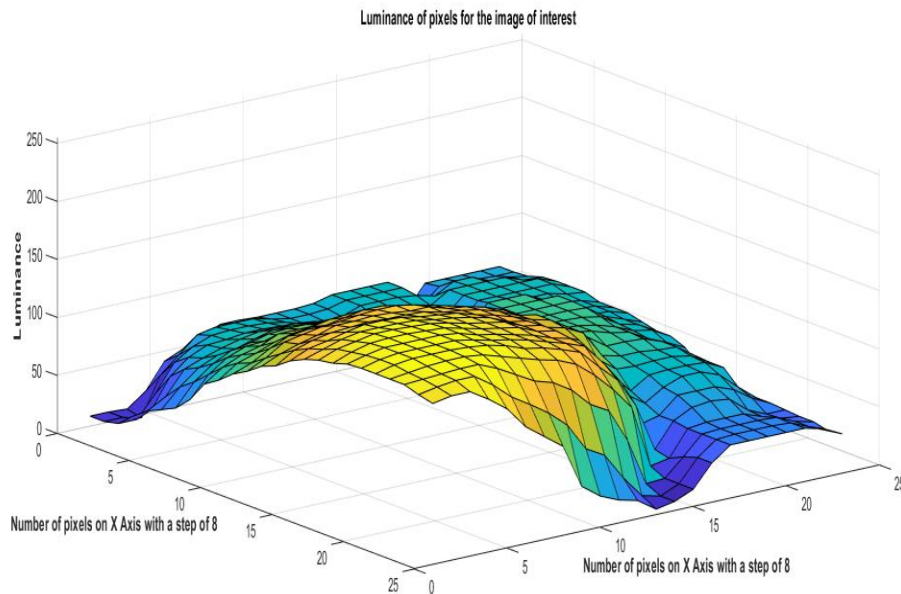


Fig. 2. Luminance of pixels for the image of interest before background adjustment

As it can be seen in Fig. 2, the luminance of background is greater in the bottom right part. The image uses indexing syntax to view only 1 out of 8 pixels in each direction, otherwise, the surface plot would be too dense. The effects of the adjustment can be observed below, in Fig. 3, where the luminance of the pixels for the image of interest is shown.

After the adjustment is done the background approximation image is subtracted from the original image and then an increase in contrast is applied by specifying contrast limits and by stretching the intensity values to fill the dynamic range. In Fig. 4, the photograph of the arteries contained in the initial image after extraction is presented.

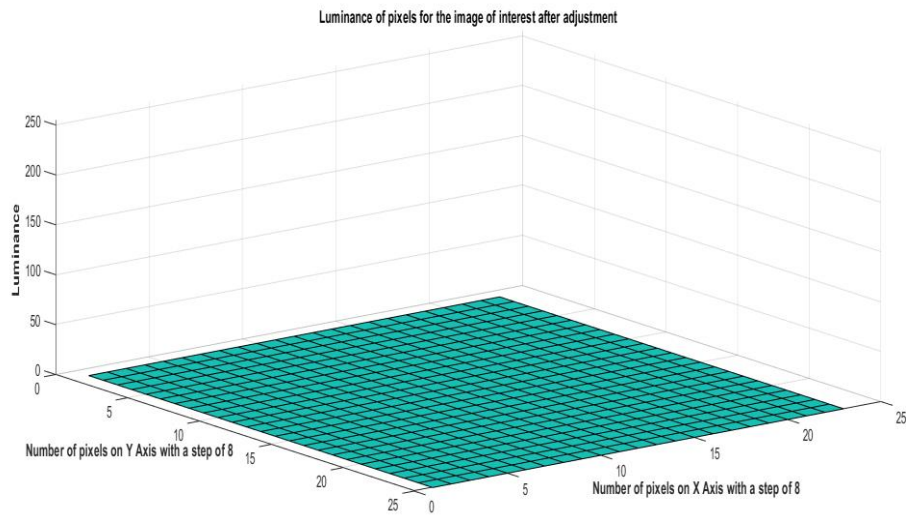


Fig. 3. Luminance of pixels for the image of interest after background adjustment

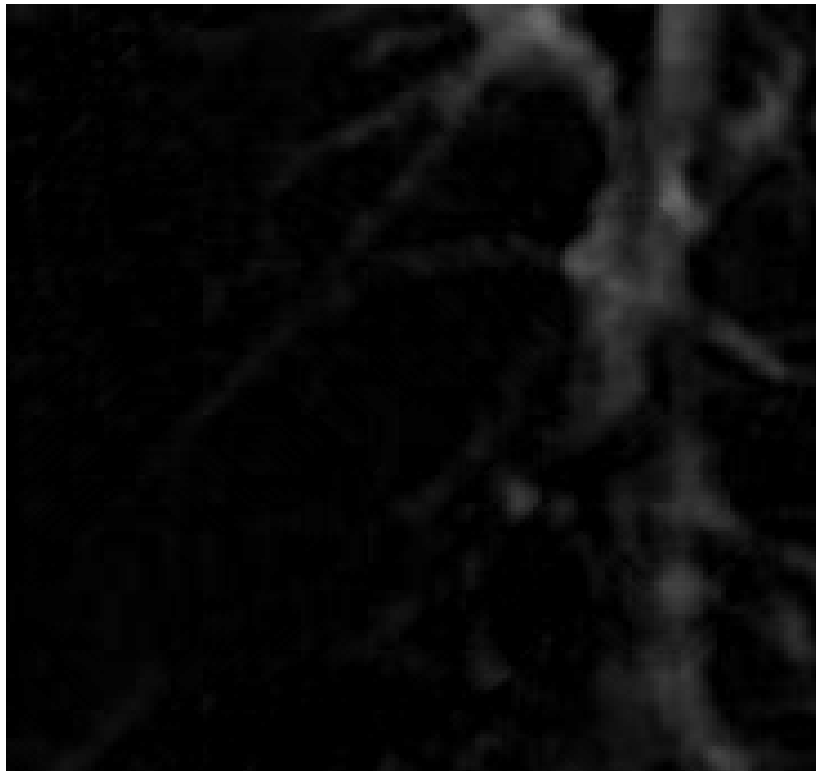


Fig. 4. The arteries contained in the initial image after extraction

Finally, the box-counting algorithm is used to determine fractal properties of the image.

Assuming there is a fractal set  $C$  that has the fractal dimension  $D_F < D$ , then the number  $N$  of boxes of size  $R$  needed to cover the set scales as  $R^{D_F}$ .  $D_F$  is known as the Minkowski-Bouligand dimension, or Kolmogorov capacity, or Kolmogorov dimension, or simply box-counting dimension [18-19].

The program developed to find out the fractal dimension for arteries shown in Fig. 4 using a function of type  $\text{boxcount}(C)$ .

$[N R] = \text{boxcount}(C)$ , where  $C$  is a  $D$ -dimensional array (with  $D=1, 2, 3$ ), counts the number  $N$  of  $D$ -dimensional boxes of size  $R$  needed to cover the nonzero elements of  $C$ . The box sizes are powers of two, i.e.,  $R = 1, 2, 4 \dots 2^P$ , where  $P$  is the smallest integer such that the maximum length present in  $C$  is smallest or at least equal with  $2^P$ . If the sizes of  $C$  over each dimension are smaller than  $2^P$ ,  $C$  is padded with zeros to size  $2^P$  over each dimension. The output vectors  $N$  and  $R$  are of size  $P+1$ . For a RGB color image ( $m$ -by- $n$ -by-3 array), a summation over the 3 RGB planes is done first [20]. To remove pixels that might have a negative influence in measurement, due to their increased luminance, the picture of interest was binarized, as it can be seen in Fig. 5.

Additionally, the function  $\text{boxcount}(C, \text{'slope'})$  was used to show the semi-log plot of the local slope  $D_F = -\text{dln}N/\text{dln}R$  as a function of  $R$ , as it can be seen in Fig. 6. If  $D_F$  is constant in a certain range of  $R$ , then  $D_F$  is the fractal dimension of the set  $C$ .



Fig. 5. Binarized image of interest



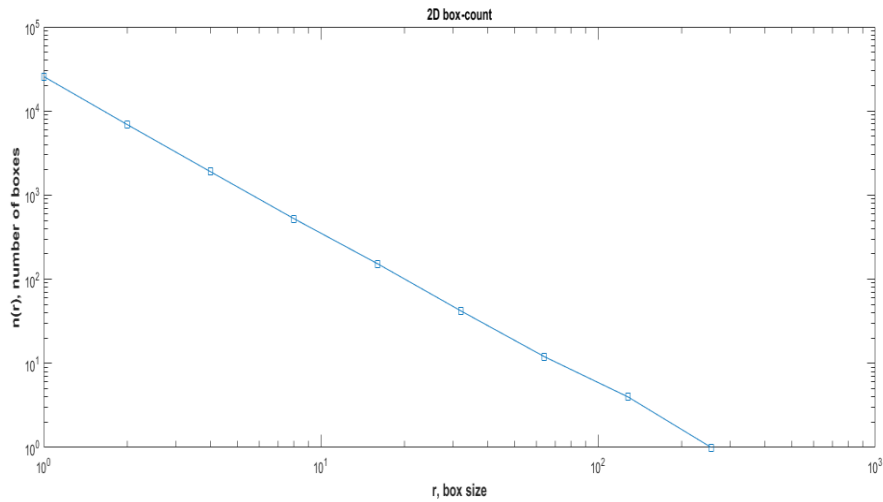


Fig. 6. Result of box-counting method

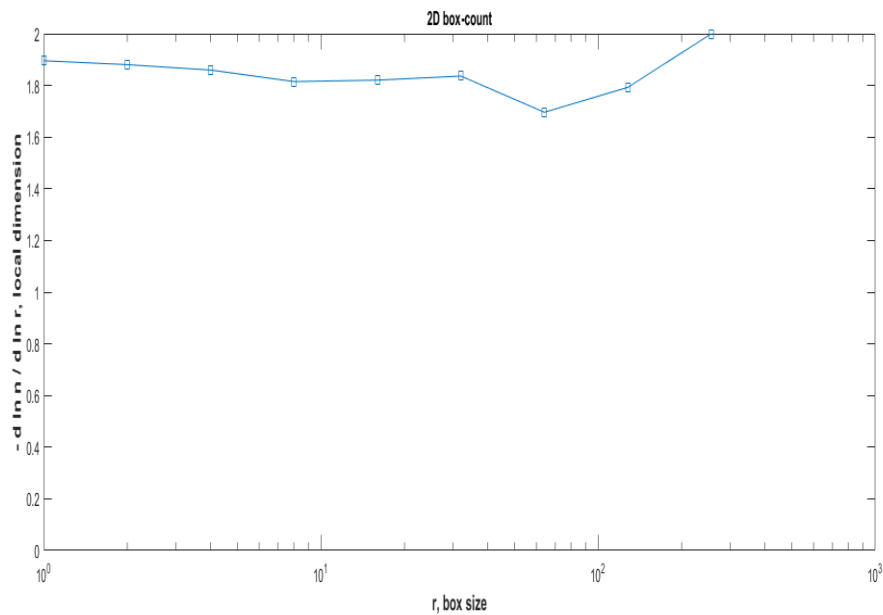


Fig. 7. Result of box-counting method with option “slope”

The result of box-counting method with the “slope” option can be visualized in Figure 7. The fractal dimension determined is equal to  $1.7086 \pm 0.17389$ .

#### 4. Box-counting algorithm with rectangular mask

The box-counting algorithm has been improved by using masks of variable size to make calculations to obtain fractal dimension and to improve the standard deviation.

In accordance with this purpose the set of five variable size masks was defined as a 5 by 2 matrix. More exactly, the frame dimensions for length and width ( $r_x$  and  $r_y$ ) were  $\{1,2\},\{2,4\},\{4,8\},\{8,16\}$  and  $\{16,32\}$  pixels. The cells were successively applied to the picture as in the original box-count algorithm.

Because of the difference between mask length and width, a 3D graph as the one in Fig. 8 was used to show the results. The figure is realized using  $\log(1/r_x)$  for the X axis,  $\log(1/r_y)$  for Y axis and  $\log(n)$  for Z axis.

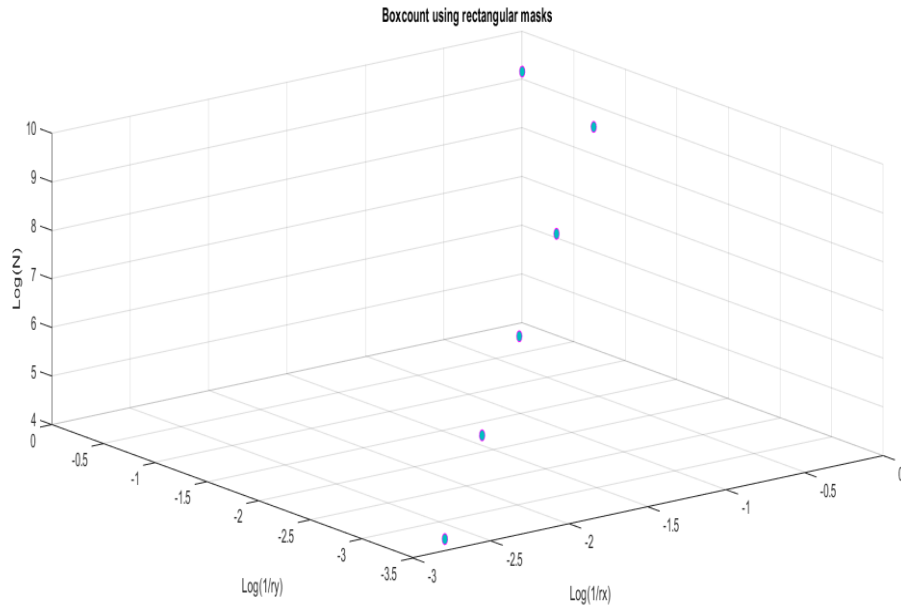


Fig. 8. Box-count algorithm using rectangular mask

The fractal dimension was obtained using the equation  $z = f(x, y)$ , with  $x = \log(1/r_x)$ ,  $y = \log(1/r_y)$  and  $f = \log(n)$ ,  $n$  being the number of  $D$ -dimensional boxes of size  $\{r_x, r_y\}$  needed to cover the nonzero elements of the binary image. Therefore, the equation that was used for square masks,  $f(x) = a + bx$ , is now adjusted to  $f(x, y) = a + bx + cy$ . The use of square boxes leads to  $x = y$  and thus  $f = a + (b + c)x$ , which means  $D=b+c$ .

$$\text{Moreover, since } b = \frac{\partial f}{\partial x} \text{ and } c = \frac{\partial f}{\partial y}, \quad (4)$$

we infer,

$$D = \frac{\partial f}{\partial x} + \frac{\partial f}{\partial y} \quad (5)$$

The adjusted algorithm provides the fractal dimension

$$D = 1.5661 \pm 0.11691 \quad (6)$$

## 5. Comparing MATLAB results with HarFa results

In order to compare and check the results, the algorithm was also performed in Harmonic and Fractal Image Analyzer Demo version 5.5.30.

The first step consisted in loading the image shown in Fig. 4 and preparing it for transformation into binary format by setting the intensity threshold between 9 and 255. This means that all pixels that exceed this value will get the white color and the others will get the black color. The action is enabled by pressing the "Perform Thresholding" button. The image preparation for analysis can be seen in Fig. 9.

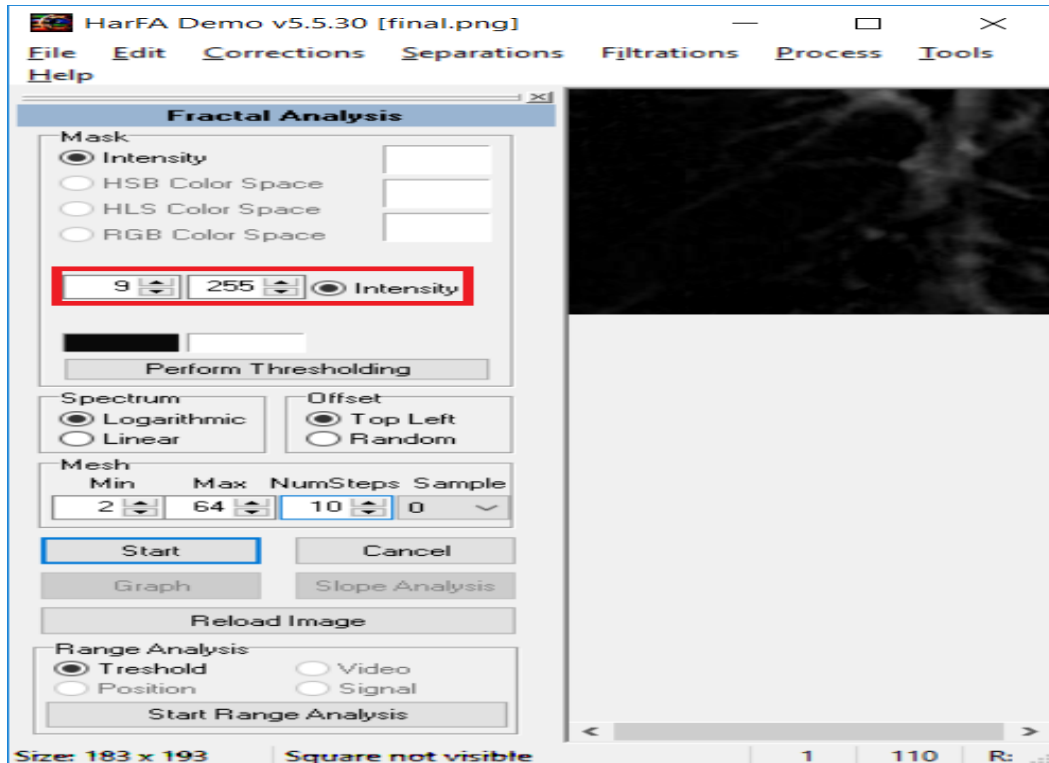


Fig. 9. Prepare image of interest to analyze

Further, the "Start" button is pressed and the box-count method is applied. Then, the program returns the graph containing the fractal analysis from which the line equation leads to

$$y = 1.6346x + 0.3333 \quad (7)$$

The fractal spectrum can be displayed by pressing the “Start Range Analysis” button in the main window. In Fig. 10 one can see the image of interest in binary format.

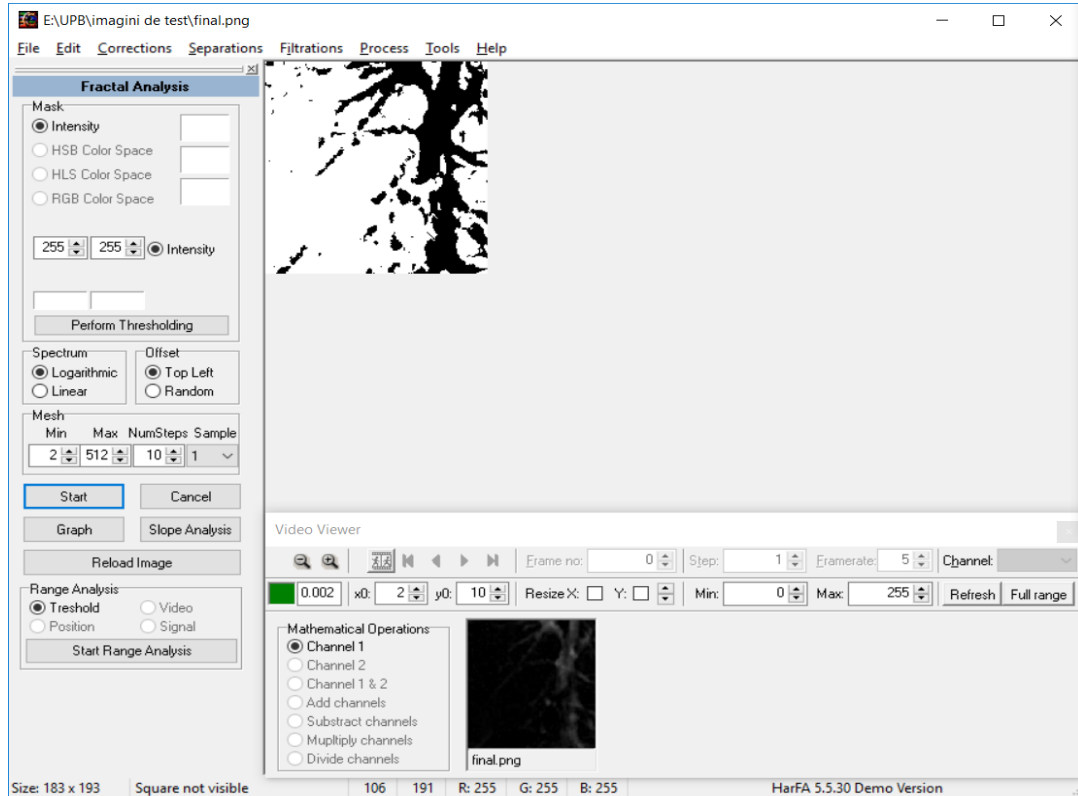


Fig. 10. The image of interest in binary format

In Fig. 11 the window for fractal analysis is depicted, showing the various features of the program, such as the number of squares and scale selection as well as giving us the statistics of the data used. In this figure,  $\ln(N)$  as a function of  $\ln(r)$  is obtained. Finally, in Fig. 12, the fractal spectrum is presented, which gives useful information about the fractal dimension versus intensity.

As it can be seen in the figures below (Figs. 11 and 12), the results are almost the same in both pieces of software, MATLAB R2017a and Harmonic and Fractal Image Analyzer Demo version 5.5.30 respectively.

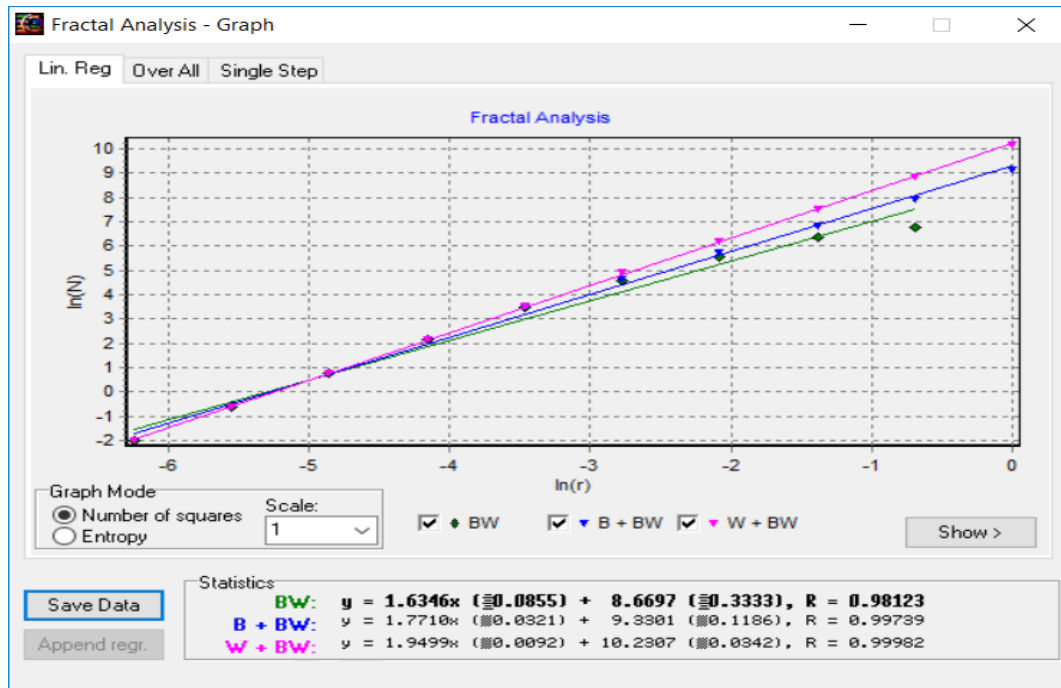


Fig. 11. Fractal analysis

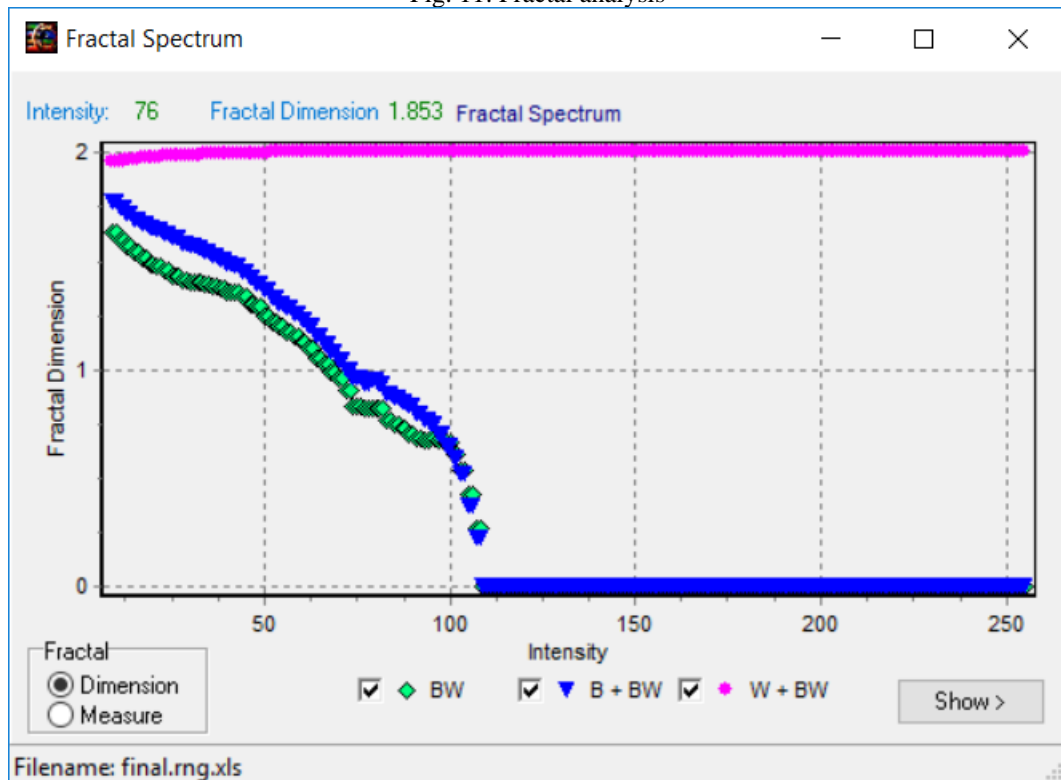


Fig. 12. Fractal spectrum

## 6. Conclusions and future work

In this paper a pulmonary radiograph was analyzed to find out the fractal dimension of a pulmonary artery. For this purpose, the radiograph was processed in MATLAB R2017a to remove lung and just keep the artery. Then, the image was transformed into binary format and the box-count method was applied to reach the results.

In order to improve the measurements a variable size mask was adopted. It is represented by a 5-by-2 matrix on whose rows the cells are defined. In each iteration a mask is taken, and the original image is covered. At the end of this kind of algorithm an improvement in standard deviation is obtained.

Finally, the comparison between the results obtained in MATLAB environment and Harmonic and Fractal Image Analyzer Demo version 5.5.30 software showed almost no difference.

As an observation, it can be mentioned that the resolution of the initial image brings significant influence on the entire analysis process due to the noise it can present, and which is sometimes quite difficult to remove.

The software developed in this paper can be fully integrated into a medical equipment which can be used in detection and monitoring of lung diseases or other organs.

Further research can be made in the future when additional results can be obtained by improving the initial imaging process and performing the detailed detection of the areas affected by the tumors.

## REFERENCES

- [1]. *B. Mandelbrot*, Fractal geometry of nature, Freeman, New York, 1983, pp. 25-57
- [2]. *C. A. Rogers*, Hausdorff Measures, Cambridge University Press, Oxford, 1970
- [3]. *M. Agop, P. E. Nica, S. Gurlui, C. Focsa, V. P. Paun, M. Colotin*, Implications of an extended fractal hydrodynamic model, European Physical Journal D, vol. **56**, no.3, 2010, pp. 405-419
- [4]. *O. Niculescu, D. G. Dimitriu, V. P. Paun, P. D. Matasaru, et al.*, Experimental and theoretical investigations of a plasma fireball dynamics, Physics of Plasmas/Phys. Plasmas, vol. **17**, no.4, 2010, Article Number: 042305
- [5]. *Michinobu Nagao, Kenya Murase, Takanori Kikuchi, Manabu Ikeda, Akihiko Nebu, Ryuji Fukuhara, Yoshifumi Sugawara, Hitoshi Miki and Junpei Ikezoe*, Fractal Analysis of Cerebral Blood Flow Distribution in Alzheimer's Disease, J Nucl Med., vol. **42**, 2001, pp. 1446-1450
- [6]. *Khan M. Iftekharruddin, W. Jia, R. Marsh*, Fractal analysis of tumor in brain MR images, Machine Vision and Applications, vol. **13**, 2003, pp. 352-362
- [7]. *M. Honciuc, V. P. Paun*, Liquid crystal-like behavior of some fatty acids mixtures, Revista de Chimie, vol. **54**, no.1, 2003, pp.74-76
- [8]. *S. Pusca, M. A. Paun, C. Toma*, Viscoelastic behaviour analysis of the technical polymers by bidimensional pulses generation, Materiale Plastice, vol. **44**, no.1, 2007, pp.39-42

- 
- [9]. *D. Iordache, S. Pusca, G. Toma, G., V.P. Paun, A. Sterian, C. Morarescu*, Analysis of compatibility with experimental data of Fractal descriptions of the fracture parameters, *Lect Notes Comput SC* vol. **3980**, 2006, pp. 804-813
- [10]. *M. Olteanu, V. P. Paun, M. Tanase*, Fractal analysis of zircaloy-4 fracture surface, *Revista de Chimie*, vol. **56**, no. 1, 2005, pp. 97-100
- [11]. *Z. Borsos, V. P. Paun, I. Casian-Botez, et al.*, Structural Conductivity of Carbon Nanotubes, *Revista de Chimie*, vol. **59**, no. 10, 2008, pp. 1169-1171
- [12]. *R. Stana, I. Casian Botez, V. P. Paun, et al.*, New Model for Heat Transfer in Nanostructures, *Journal of Computational and Theoretical Nanoscience*, vol. **9**, no. 1, 2012, pp. 55-66
- [13]. *V. P. Paun*, Fractal surface analysis of the Zircaloy-4 SEM micrographs by time series method, *Central European Journal of Physics*, vol. **7**, no. 2, 2009, pp. 264-269
- [14]. *P. Postolache, L. D. Duceac, E. G. Vasincu, M. Agop, R. M. Nemes*, Chaos and Self-Structuring Behaviors in Lung Airways, *University Politehnica of Bucharest Scientific Bulletin-Series A-Applied Mathematics and Physics*, vol. **78**, no. 1, 2016, pp. 291-298
- [15]. *P. Postolache, Z. Borsos, V. A. Paun, V. P. Paun*, New Way in Fractal Analysis of Pulmonary Medical Images, *University Politehnica of Bucharest Scientific Bulletin-Series A-Applied Mathematics and Physics*, vol. **80**, no.1, 2018, pp. 313-322
- [16]. *K. M. Iftekharuddin, W. Jia, R. Marsh*, Fractal analysis of tumor in brain MR images, *Machine Vision and Applications*, vol. **13**, 2003, pp. 352-362
- [17]. [https://www.mathworks.com/help/images/image-enhancement-and-analysis.html?searchHighlight=analyze%20grayscale&s\\_tid=doc\\_srchtile](https://www.mathworks.com/help/images/image-enhancement-and-analysis.html?searchHighlight=analyze%20grayscale&s_tid=doc_srchtile)
- [18]. *K. Mehlhorn, S. Naher*, LEDA – A platform for combinatorial and geometric computing, Max Planck Institut fur Informatik, Saarbrucken, Germany
- [19]. *S. Arianos, E. Bompard, A. Carbone, F. Xue*, Power grid vulnerability: A complex network approach, *CHAOS* 19, 2009.
- [20]. [https://www.mathworks.com/matlabcentral/fileexchange/13063-boxcount?s\\_tid=srchtitle](https://www.mathworks.com/matlabcentral/fileexchange/13063-boxcount?s_tid=srchtitle)